International Journal of Nanomedicine

Dovepress
Taylor & Francis Group

Open Access Full Text Article

ORIGINAL RESEARCH

Engineering Optimized Nanostructured Lipid Carriers for Astaxanthin: A Response Surface Methodology Approach

Nur Rafiqah Abdol Wahab[1], Meor Mohd Redzuan Meor Mohd Affandi[2], Sharida Fakurazi[1], Ekram Alias[3], Haniza Hassan[1]

[1]Department of Human Anatomy, Faculty of Medicine and Health Sciences, Universiti Putra Malaysia (UPM), Serdang, SEL, Malaysia; [2]School of Pharmacy, Puncak Alam Campus, Universiti Teknologi MARA (Uitm), Bandar Puncak Alam, SEL, Malaysia; [3]Department of Biochemistry, Faculty of Medicine, Universiti Kebangsaan Malaysia (UKM), Kuala Lumpur, Malaysia

Correspondence: Haniza Hassan, Department of Human Anatomy, Faculty of Medicine and Health Sciences, Universiti Putra Malaysia (UPM), Serdang, SEL, Malaysia, Tel +60397692665, Email nizahassan@upm.edu.my; Ekram Alias, Department of Biochemistry, Faculty of Medicine, Universiti Kebangsaan Malaysia (UKM), Jalan Yaakob Latiff, Bandar Tun Razak, Kuala Lumpur, Malaysia, Tel +60391459553, Email ekram.alias@ukm.edu.my

Introduction: The xanthophyll carotenoid astaxanthin is well-known for its potent antioxidant properties, which are superior to those of other antioxidants such as vitamins C and E. However, this highly hydrophobic compound has low solubility and poor oral bioavailability, limiting its efficacy and clinical application. To address these pharmacokinetic challenges, nanostructured lipid carriers (NLC) have been proposed as potential lipid-based drug carriers for the oral delivery of astaxanthin owing to their excellent biocompatibility, stability, and efficient drug loading capacity.

Purpose: In this study, we aimed to develop an NLC using cocoa butter and palm oil for astaxanthin encapsulation, and to optimize the nanoformulation by employing Response Surface Methodology (RSM), a statistical approach.

Methods: Three-factor Central Composite Design (CCD) in RSM was used to understand the effect of independent variables on response variables. The size, polydispersity index, and encapsulation efficiency of the astaxanthin-loaded NLC were also characterized.

Results: Findings of this study indicated that the mass of cocoa butter, palm oil and Tween 80 influenced the particle size, polydispersity index and zeta potential of NLC. The experimental determination of NLC did not differ significantly from the predicted RSM outcomes with size, polydispersity index and zeta potential of 254.42 ± 3.91 nm, 0.38 ± 0.01 and −30.54 ± 0.85 mV, respectively. This nanoparticulate system showed an excellent astaxanthin entrapment efficiency of 99.69±0.0003%.

Conclusion: The ideal combination of each composition in the NLC formulation yielded nanoparticles with desirable particle size, polydispersity index, and zeta potential for efficient oral delivery of astaxanthin.

Plain Language Summary: Astaxanthin is a natural antioxidant that is much stronger than vitamins C and E. However, it does not dissolve well in water and is poorly absorbed when administered orally, which limits its usefulness. To overcome this drawback, this study explored the use of nanostructured lipid carriers (NLC), which are tiny fat-based particles, to improve astaxanthin movement in the body.

An NLC formulation was developed using cocoa butter and palm oil. The optimization process was conducted using a statistical method called Response Surface Methodology (RSM) to determine the best combination of ingredients.

Different amounts of cocoa butter, palm oil, and a stabilizer (Tween 80) can affect the size, stability, and ability of the particles to hold astaxanthin. The results also showed that the optimized NLC had a small and uniform size (approximately 254 nm), stable dispersion (zeta potential of −30.54 mV), and highly efficient astaxanthin trapping (99.69%).

In conclusion, we successfully developed an NLC formulation that can efficiently carry astaxanthin, potentially improving its absorption and effectiveness when used as a supplement or medicine.

Keywords: astaxanthin, nanoformulation, drug delivery, nanostructured lipid carriers, response surface methodology, central composite design

Received: 1 June 2025
Accepted: 26 November 2025
Published: 23 December 2025

Introduction

Astaxanthin, a marine xanthophyll carotenoid, is abundant in various aquatic animals, such as shrimp, salmon, as well as algae, and yeast. This compound possesses potent and superior antioxidant activity, surpassing other carotenoids, especially beta-carotene, and antioxidant-rich vitamins C and E.[1] This fat-soluble nutrient has garnered significant interest with numerous ongoing studies investigating the health effects of astaxanthin as nutraceuticals.[2,3] For instance, in a human trial conducted in Japan, it was found that daily intake of 9 mg of astaxanthin for 12 weeks improved composite and verbal memory in 44 adult volunteers. It has been suggested that declines in cognitive function due to nerve cell damage caused by oxidative stress could be improved by astaxanthin supplementation.[4] Apart from the beneficial effects of astaxanthin on cognitive function and anti-aging, Zhuge et al (2021) discovered that daily consumption of astaxanthin could help lower blood glucose and total cholesterol levels in diabetes-induced rats after a 3-week treatment. They reported that the astaxanthin-treated group had higher expression of insulin-related genes, such as adiponectin, adiponectin receptor 1, and adiponectin receptor 2, which explained the blood glucose-lowering effect and ameliorated insulin resistance in the type-2 diabetes mellitus rats.[5] Furthermore, a more recent bone-related health study by Chang et al (2022) concluded that astaxanthin could reduce the accumulation of reactive oxygen species in damaged bone cells and promote bone remodeling. Astaxanthin suppressed the production of cyclooxygenase-2 (COX-2) and nitric oxide, which are usually expressed during inflammation in damaged bone cells. This has led to a reduction in the oxidative damage caused by excessive free radicals and inflammation, which subsequently promoted new bone cell formation.[6]

Despite the promising pharmacological effects of astaxanthin, its poor pharmacokinetic profile hinders its clinical application.[7] The oral bioavailability of astaxanthin is poor, ranging between 10–50% of the administered dose. Besides that, the maximum plasma concentration (C_{max}) and volume of distribution of free astaxanthin after a single dose of 100 mg/kg were also reported very low, about 1.3 ± 0.1 mg/L and 0.40 ± 0.2 L/kg, respectively. In addition, the time required for astaxanthin to reach its peak plasma concentration was quite long, between 6 and 7 h, and the half-life elimination was approximately 21 ± 11 h after oral administration.[8]

To overcome these pharmacokinetic challenges, various strategies have been designed and attempted. For example, Okada et al (2009) suggested that the consumption of astaxanthin after meals could enhance its oral bioavailability by 2.5 times as compared to that in the group of volunteers who consumed it before meal.[9] They postulated that this finding could be due to the presence of lipids in the meal, which help enhance the absorption of astaxanthin. Prior to this study, Odeberg et al (2003) demonstrated that incorporating astaxanthin into a lipid-based formulation consisting of glycerol mono- and di-oleate improved the solubility and oral bioavailability of astaxanthin by 3.7 times when compared to the reference formulation made of algae and dextrin encapsulated in hard-shelled capsules.[7] Therefore, it is rational to develop a cost-effective lipid-based drug carrier system composed of Generally Recognized As Safe (GRAS) ingredients with the aim of enhancing the oral pharmacokinetic profile of astaxanthin.

In the last decade, several nanodrug delivery systems including nanoemulsions, liposomes, and solid lipid nanoparticles (SLN) have been developed to incorporate astaxanthin for oral delivery. These nanoformulations have been proven to enhance compound stability and improve oral bioavailability in addition to their efficacy.[10] However, nanoemulsions have been reported to separate over time and reduce stability during shelf storage, whereas liposomes have low drug or active compound encapsulation efficiency, and the SLN system may cause drug leakage during storage.[2,11] Therefore, the use of a new generation of lipid-based nanoparticles, nanostructured lipid carriers (NLC), has been proposed as a promising strategy.[12]

NLCs consist of a lipid core, surfactant, and aqueous phase. The lipid core is made of a mixture of solid lipid such as cocoa butter and liquid lipid that intended to produce an imperfect lipid arrangement to allow efficient drug loading and provide stability during storage.[13–15] Commonly, liquid lipids used in NLC formulations include vegetable oils that consist of mono-, di-, and triglycerides, containing fatty acids. Palm oil is one of the examples that contains many phytonutrients and has been shown to improve the stability of various active pharmaceutical ingredients.[16] Blending solid lipids with vegetable oil also enables the encapsulation of drugs with bulky structures, such as astaxanthin.[17] In addition to lipids, one of the most commonly used food-grade surfactants in various formulations is Tween 80, because of its efficient emulsifying ability.[18] Most importantly, an optimum combination of these main ingredients in the NLC formulation should be considered to ensure the production of nano-sized particles with good physicochemical properties. Also, there are limited formulations of

astaxanthin-loaded NLC with appropriate particle size, polydispersity index as well as encapsulation efficiency. For example, Radić et al (2023) reported the entrapment efficiency for astaxanthin-loaded NLC was only 58.0%.[19] The result reflected may be due to lack of optimization strategies upon formulating the NLC. Therefore, optimization is a crucial step in nanoformulation development to determine the composition of each ingredient.

Conventionally, most studies employ the one-factor-at-a-time (OFAT) approach for optimization, whereby researchers can only change a single factor or variable while keeping the other independent variables constant at one time. This method often relies on fixed assumptions and linear relationships, which can limit its effectiveness under complex scenarios. In addition, this study design often requires a large amount of resources and the results can be misinterpreted.[20] Conversely, a widely used technique for modelling and analyzing processes that explores different relationships between all variables and their responses simultaneously, such as Response Surface Methodology (RSM), should be explored. This dynamic approach allows researchers to gain deeper insights and achieve better results, particularly in fields that require meticulous analyses and adaptability. Several experimental studies have optimized efficient nanocarriers by employing the Central Composite Design (CCD) in RSM such as optimized-Nano-Hydroxyapatite loaded with tocotrienol-rich fraction (TRF) as well as optimized SLN incorporated with acyclovir.[20,21] CCD has been successfully employed to optimize various nanoformulations such as SLN and liposome.[20] It is a common fractional factorial design used in the RSM that consists of center points augmented with a group of axial points.[22] This approach allows the optimization and explanation of response variables more effectively than the traditional OFAT approach.[20]

The innovative application of RSM for the optimization of astaxanthin-loaded nanostructured lipid carriers represents a significant advancement in the field. This approach allows for a systematic exploration of the interactions between various formulation parameters, ultimately enhancing the efficiency and effectiveness of the delivery system. By employing this methodology, we can identify optimal conditions that maximize the encapsulation and stability of astaxanthin, thereby improving its bioavailability and therapeutic potential. Also, we aimed to determine the association between independent variables and response variables, such as particle size, polydispersity index (PdI), and zeta (ζ) potential of the NLC formulation developed using palm oil and cocoa butter. The response variables are important Critical Quality Attribute (CQA) to be optimized for NLC formulation, as it influences the effectiveness of the formulation such as dissolution, solubility and most importantly the oral bioavailability.[23] Additionally, these particles are expected to exhibit high encapsulation efficiency, ensuring that the desired substances are effectively delivered and retained within the nanoparticle system.

Materials and Methods

Materials

AstaReal® L10, 10% w/w standardized astaxanthin derived from *Haematococcus pluvialis* was gifted by Fuji Chemical (Fuji Chemical Industry Co., Ltd., Japan) and obtained from its sole distributor, Elite Organic Sdn Bhd (Kuala Lumpur, Malaysia). Cocoa butter was sponsored by the Guan Chong Cocoa Manufacturer, Sdn Bhd (Johor, Malaysia). Palm oil was purchased from SD Guthrie (Kuala Lumpur, Malaysia) and Tween 80 was obtained from Chemiz (M) Sdn Bhd. All other chemicals used in this study were of analytical grade unless otherwise stated.

Central Composite Design

The experimental design, statistical analysis, model selection, and numerical optimization were conducted using a software, Design-Expert® (Ver. 6.0.6, Stat-Ease, Inc., Minnesota, USA). A Central Composite Design with a three-factor experimental model consisting of 20 runs that were generated by the software, was employed to optimize the formulation composition. The masses of cocoa butter (A, g), palm oil (B, g), and Tween 80 (C, g) were chosen as independent variables, while the response variables were particle size (Y1, nm), PdI (Y2), and ζ-potential (Y3, mV). The experimental level for each variable was chosen based on preliminary studies.[24,25] The ranges of these variables are listed in Table 1. Significant differences between independent variables were analyzed using ANOVA, and all significant variables were included in the final model. The interactions between variables and responses were visualized in three-dimensional (3D) response surface plots. A good fit model was represented by R^2 values of greater than 0.8.

Table 1 The Independent and Dependent Variables and Their Levels for Central Composite Design

Variable, Unit	Factors	Level		
	X	−1	0	+1
Independent variables				
Cocoa butter, solid lipid (g)	A	5	6.75	8.5
Palm oil, liquid lipid (g)	B	1.5	3.25	5
Tween 80, surfactant (g)	C	1	1.5	2
Dependent variables		**Optimized response**		
Particle size (nm)	Y1	Minimize		
Polydispersity index, PdI	Y2	In range		
Zeta potential, ζ (mV)	Y3	In range		

The polynomial equation was as follows:

$$Y = \beta_0 + \beta_1 A + \beta_2 A^2 + \beta_3 B + \beta_4 B^2 + \beta_5 C + \beta_6 C^2 + \beta_7 AB + \beta_8 AC + \beta_9 BC \quad (1)$$

where Y is the individual dependent variable; β_1-β_9 are the coefficients associated with each variable; and A, B, and C are the independent variables. Equation (1) was used to validate and establish the final reduced model, and the experimental and predicted values were compared.

Verification of the Models

Independent *t*-test was conducted between the predicted values and experimental values to validate and establish the final reduced model. $p<0.05$ was considered statistically significant.

Preparation of Blank NLC

NLC was prepared by employing hot high-shear homogenization combined with ultrasonication, following the techniques of Naseri et al (2015) and Rohmah et al (2020) with slight modification.[14,25] Cocoa butter, palm oil, and Tween 80 were weighed according to the composition generated by CCD (Table 2), and an appropriate amount of deionized water was added to make up 100 g of the overall formulation. Palm oil, deionized water, and Tween 80 were heated to 40°C, while cocoa butter was melted using a double-boiling method. Both lipids were combined prior to dispersion in the aqueous phase, which contained deionized water and Tween 80, at a speed of 1000 rpm for 10 min and maintained temperature of 40°C. For astaxanthin-loaded NLC, 1 g of Astareal® was added to the blended lipids, following previous studies.[26,27] The mixture was emulsified using a high-speed homogenizer (PRO Scientific, PRO400DS, USA) at 20,000 rpm for 20 min. Finally, ultrasonication was performed for 5 min at 40% amplitude using an ultrasonicator with a probe before allowing the astaxanthin-loaded NLC to cool down to room temperature (25°C ± 2°C) for recrystallization.

Particle Size, Polydispersity and Zeta (ζ) Potential

The particle size, PdI, and ζ-potential of the astaxanthin-loaded NLC formulation were determined by dynamic light scattering (DLS) technique using a particle size analyzer (Zetasizer Nano ZS, Malvern Instruments, Malvern, UK). Prior to the analysis, the formulation was diluted with deionized water to avoid multiple scattering effects. The samples were carried out in triplicate at an angle of 90° in 0.01m width cells at 25.0 ±0.1 °C.

Transmission Electron Microscopy (TEM)

Morphological analysis of the astaxanthin-loaded NLC and blank NLC was performed using TEM (JEM-2100F, JEOL, Tokyo, Japan). One drop of the dispersed nanoparticles was placed on a carbon-coated grid, stained with a saturated solution of uranyl acetate, and air-dried at room temperature before analysis. The test was carried out at room temperature (25 ± 1 °C).

Table 2 Experimental Central Composite Design (CCD) and Observed Response Value

Run	Type	Independent Variables			Dependent Variables		
		Cocoa Butter (g)	Palm Oil (g)	Tween 80 (g)	Particle Size (nm)	Polydispersity Index	Zeta Potential (mV)
		A	B	C	Y1	Y2	Y3
1	**Center**	**6.75**	**3.25**	**1.50**	**207.0**	**0.325**	**−29.8**
2	Axial	6.75	3.25	2.34	185.4	0.258	−27.3
3	Fact	8.50	1.50	1.00	385.5	0.405	−34.4
4	Axial	3.81	3.25	1.50	230.5	0.371	−25.3
5	Fact	5.00	1.50	1.00	239.5	0.486	−33.7
6	Fact	8.50	1.50	2.00	214.1	0.462	−25.1
7	**Center**	**6.75**	**3.25**	**1.50**	**202.8**	**0.305**	**−32.1**
8	Fact	5.00	5.00	2.00	236.5	0.267	−25.2
9	**Center**	**6.75**	**3.25**	**1.50**	**215.0**	**0.345**	**−30.6**
10	**Center**	**6.75**	**3.25**	**1.50**	**200.0**	**0.258**	**−20.3**
11	Axial	6.75	3.25	0.66	246.2	0.405	−27.3
12	Fact	8.50	5.00	2.00	207.0	0.251	−34.5
13	Fact	5.00	1.50	2.00	201.9	0.442	−33.0
14	Axial	9.69	3.25	1.50	236.9	0.327	−31.9
15	**Center**	**6.75**	**3.25**	**1.50**	**240.8**	**0.386**	**−32.3**
16	**Center**	**6.75**	**3.25**	**1.50**	**201.5**	**0.307**	**−23.5**
17	Fact	8.50	5.00	1.00	253.8	0.354	−37.1
18	Fact	5.00	5.00	1.00	242.5	0.423	−36.7
19	Axial	6.75	6.19	1.50	395.0	0.489	−32.2
20	Axial	6.75	0.31	1.50	228.8	0.475	−49.3

Notes: Six center points were highlighted in gray and presented in bold font.

Entrapment Efficiency (EE)

The entrapment efficiency capacity were determined following a previously described method with some modifications.[21,25] 3 mL of astaxanthin-loaded NLC filled in centrifugal filter tubes (Amicon® Ultra-4, Sigma-Aldrich, Massachusetts, USA) was centrifuged using a multifunction centrifuge with a fixed 23° angle rotor at 5000 rpm for 30 min at 25 °C, separating the water phase from the lipid phase. The amount of unloaded astaxanthin was analyzed using a UV spectrophotometer at a wavelength of 492 nm.[28] Quantification of astaxanthin was performed by preparing a calibration curve using a linear regression equation. Entrapment efficiency was calculated using Equation (2).

$$\%EE = \frac{(amount\ of\ astaxanthin - amount\ of\ unentrapped\ astaxanthin)}{amount\ of\ astaxanthin} \times 100\% \quad (2)$$

https://doi.org/10.2147/IJN.S544064

Storage Stability Determination

The formulation stability during storage was determined by transferring fresh samples into amber glass bottles immediately after the preparation, following previous studies.[19,20] This study was performed to assess the stability of the blank NLC and astaxanthin-loaded NLC, in three different temperatures; refrigerated temperature (4 ± 2 °C), room temperature (25 ± 2 °C) and accelerated temperature (40 ± 2 °C). The particle size, polydispersity index and zeta potential were measured and analyzed by using the DLS monthly for over 3 months. All measurements were repeated in triplicate.

Statistical Analysis

Statistical analyses were performed using GraphPad Prism Software (ver. 10, USA). Data are expressed as standard error of the mean (SEM). Statistical significance of the results was evaluated using an independent *t*-test to compare the two samples. A p-value of < 0.05 was considered as not significant.

Results and Discussion

Fitting the Response Surface Model

Twenty randomized experiments were conducted with six identical center points to ensure the prediction efficiency of the optimization process. The mean particle size, polydispersity index and zeta potential are listed in Table 2. The size of the produced nanoparticles ranged from 185.4 to 395 nm, while the polydispersity index was between 0.251 and 0.489. All experiments yielded zeta potentials with negative values between −49.3 to −20.3 mV.

All data were statistically analyzed, and the best-fit model for the independent variables was determined using regression equations, coefficients of multiple determinations (R^2), adequate precision values, F-values, probability values (p-values), and p-values for the lack-of-fit in Table 3. In addition, positive values in the equation indicate a synergistic effect in the regression model, whereas negative values indicate an antagonistic effect.[29] All factors showed a significant effect on particle size, with a p-value <0.001, and polydispersity index and zeta potential, with a p-value <0.05. These factors also showed high R^2 values ($R^2>0.8$), indicating that the quadratic polynomial models were adequate and significant for visualizing the actual interaction between the independent and dependent variables.[30] The R^2 values for particle size, polydispersity index, and zeta potential were 0.9750, 0.9226, and 0.8282, respectively. These values suggest that the model can predict up to 97.5% of the particle size, 92.26% of the polydispersity index, and 82.82% of the zeta potential, resulting in a strong correlation between the independent and dependent variables. The value of adequate precision measures the signal-to-noise ratio, where a ratio greater than 4 is desirable.[25] Adequate precision values for particle size, polydispersity index, and zeta potential were 16.136, 7.124, and 7.889, respectively. In addition, the p-values for the lack of fit related to all dependent variables were high ($p>0.3$), indicating that the model had a good fit. Thus, the values indicated that the quadratic model was best fitted to all responses studied.

Among the factors in the equation, A, A^2, B^2, BC, B^3, C^3 and ABC had positive coefficient values, indicating a positive effect on the particle size in the formulation. However, the negative coefficient values for factors B, C, C^2, AB, AC, and A^3 showed a passive effect on particle size, which means that as the independent variable increased, the dependent variable tended to decrease.

Factors A^2, B^2, C^2, AC, A^3 and B^3 positively influenced the polydispersity index of the nanoformulation. The mass of palm oil was a crucial factor with a p-value of 0.0055, suggesting a highly significant influence on the polydispersity index of the NLC formulation. Finally, factors A, C, and B^3 had a positive effect on the zeta potential of nanoparticles and the mass of palm oil had the most significant effect on the zeta potential ($p< 0.05$).

Normal probability plots of the residuals for particle size, polydispersity, and zeta potential are shown in Figure 1. Most experimental data fall along a straight line, suggesting that they are normally distributed.

Influence of the Independent Variables on the Particle Size

Three-dimensional (3D) response surface plots for the interaction between the independent variables and the particle size of the NLC are shown in Figure 2. In Figure 2a, the particle size decreased as the amount of liquid lipid increased. This

Table 3 Statistical Analysis of Variance (ANOVA) of the Regression Coefficients of the Quadratic Equations for Particle Size, Polydispersity Index and Zeta Potential

Variables	Particle Size (Y1)		Polydispersity Index (Y2)		Zeta Potential (Y3)	
	F-value	p-value	F-value	p-value	F-value	p-value
Model	18.03	0.0010	5.50	0.0232	3.51	0.0429
Linear Terms						
A	7.96	0.0303	0.81	0.4023	0.062	0.8100
B	25.54	0.0023	17.90	0.0055	3.12	0.1154
C	19.52	0.0045	1.02	0.3507	3.85	0.0852
Quadratic Terms						
A^2	2.23	0.1863	0.72	0.4301	0.038	0.8505
B^2	68.10	0.0002	28.87	0.0017	18.41	0.0026
C^2	3.078E-003	0.9576	0.063	0.8109		
Interaction Terms						
AB	16.10	0.0070	0.046	0.8367	2.23	0.1737
AC	15.77	0.0074	1.91	0.2165	7.029E-004	0.9795
BC	12.62	0.0120	5.95	0.0505		
Other parameters						
Lack-of-fit	1.03	0.3558	0.048	0.8348	0.044	0.9865
R^2	0.9750		0.9226		0.8282	
Adequate precision	16.136		7.124		7.889	
Second order polynomial equation						
Particle Size (Y1)	$Y1 = 211.47 + 25.99A - 46.55B - 40.70C + 6.10A^2 + 33.75B^2 - 0.23C^2 - 22.02AB - 21.80AC + 19.50BC - 8.52A^3 + 33.93B^3 + 8.00C^3 + 11.60ABC$ (3)					
Polydispersity index (Y2)	$Y2 = 0.32 - 0.021A - 0.099B - 0.024C + (8.784 \times 10^{-3})A^2 + 0.056B^2 + (2.597 \times 10^{-3})C^2 - (3 \times 10^{-3})AB + 0.019AC - 0.034BC + (2.827 \times 10^{-3})A^3 + 0.036B^3 - (7.084 \times 10^{-3})C^3 - (6 \times 10^{-3})ABC$ (4)					
Zeta Potential, mV (Y3)	$Y3 = -27.87 + 0.59A - 4.19B + 4.66C - 0.20A^2 - 4.50B^2 - 2.11AB - 0.038AC - 0.90A^3 + 3.28B^3 - 1.65C^3 - 2.19ABC$ (5)					

Notes: Independent variables: A: mass of cocoa butter; B: mass of palm oil; C: mass of Tween 80.

https://doi.org/10.2147/IJN.S544064

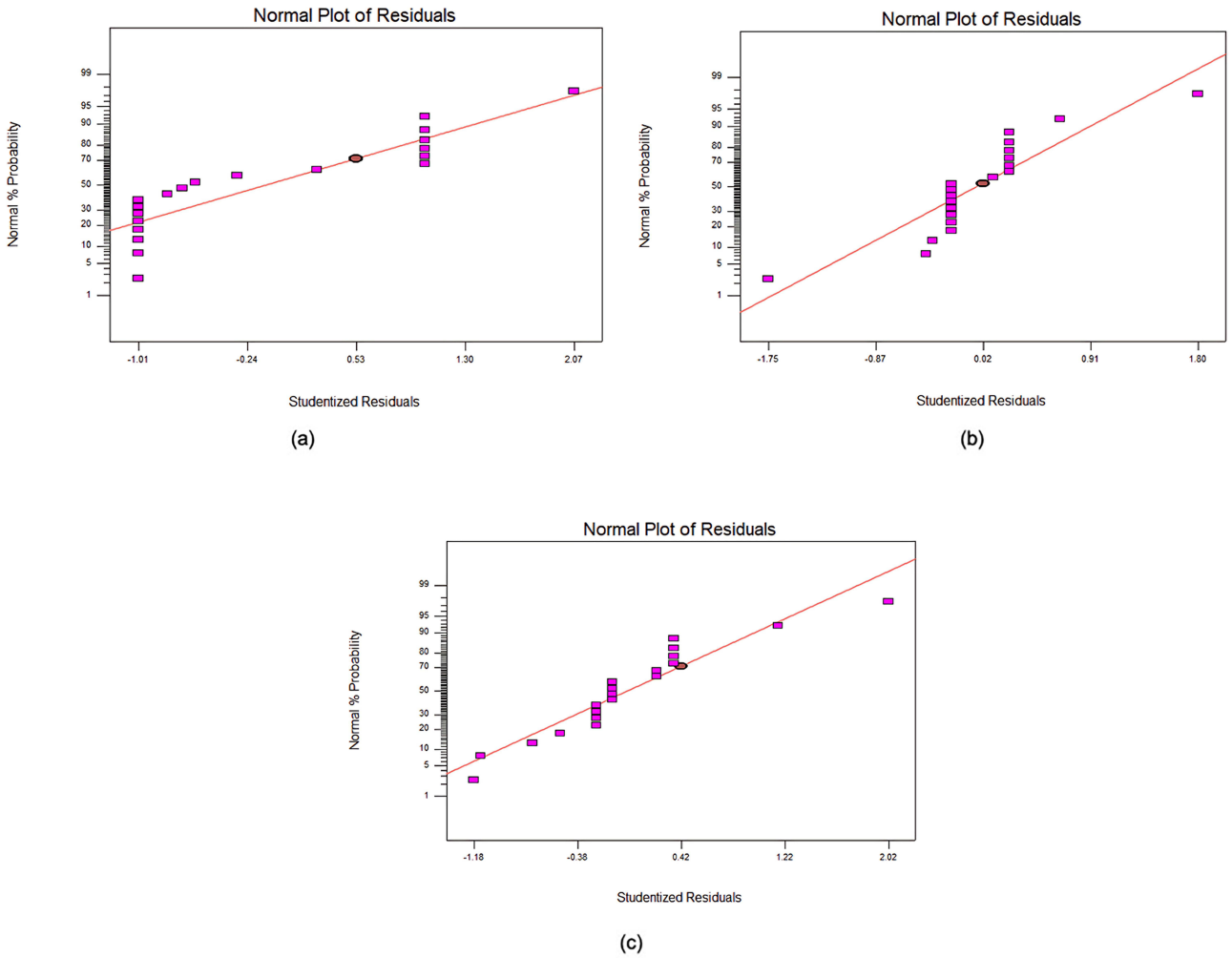

Figure 1 The normal probability plot of the residuals for **(a)** particle size, **(b)** polydispersity index and **(c)** zeta potential, indicating the normally distributed experimental values.

scenario was supported by a previous study that demonstrated liquid lipid facilitated the dispersion of the particles and improved the interaction between the particles and the solvent.[12] Based on the plot (Figure 2b), the particle size increased as the mass of solid lipids increased. Several factors may contribute to this finding. First, as the viscosity of the dispersion increased, the dispersion energy available to the system became insufficient. This phenomenon affects the shearing capacity, causing difficulty in properly homogenizing the formulation and resulting in the formation of larger particle size.[31,32] Moreover, the insufficient amount of surfactants added to the formulation to stabilize the dispersion could also be one of the factors contributing to the formation of larger particles, as seen in Figure 2c. Surfactants play an important role in reducing the surface tension between two dispersion phases.[33,34] Therefore, an adequate amount of Tween 80 is necessary for this formulation to ensure that nanosized particles are produced.

Influence of the Independent Variables on the Polydispersity Index

Figure 3 shows that increasing the mass of palm oil gradually reduced the polydispersity index, while there was minimal change with different masses of cocoa butter (Figure 3a). Similar to previous studies, a higher polydispersity index was caused by an increased amount of lipids, especially solid lipids, in the NLC.[35] This could be due to an increase in the viscosity of the formulation, which leads to uneven formation of particle shape, size and distribution.[25,34] The plot in Figure 3b also reveals that the polydispersity index of the sample decreased at a higher liquid lipid mass. This could be due to the low viscosity of the NLC dispersion when an increasing mass of liquid lipid was added, which reduced the

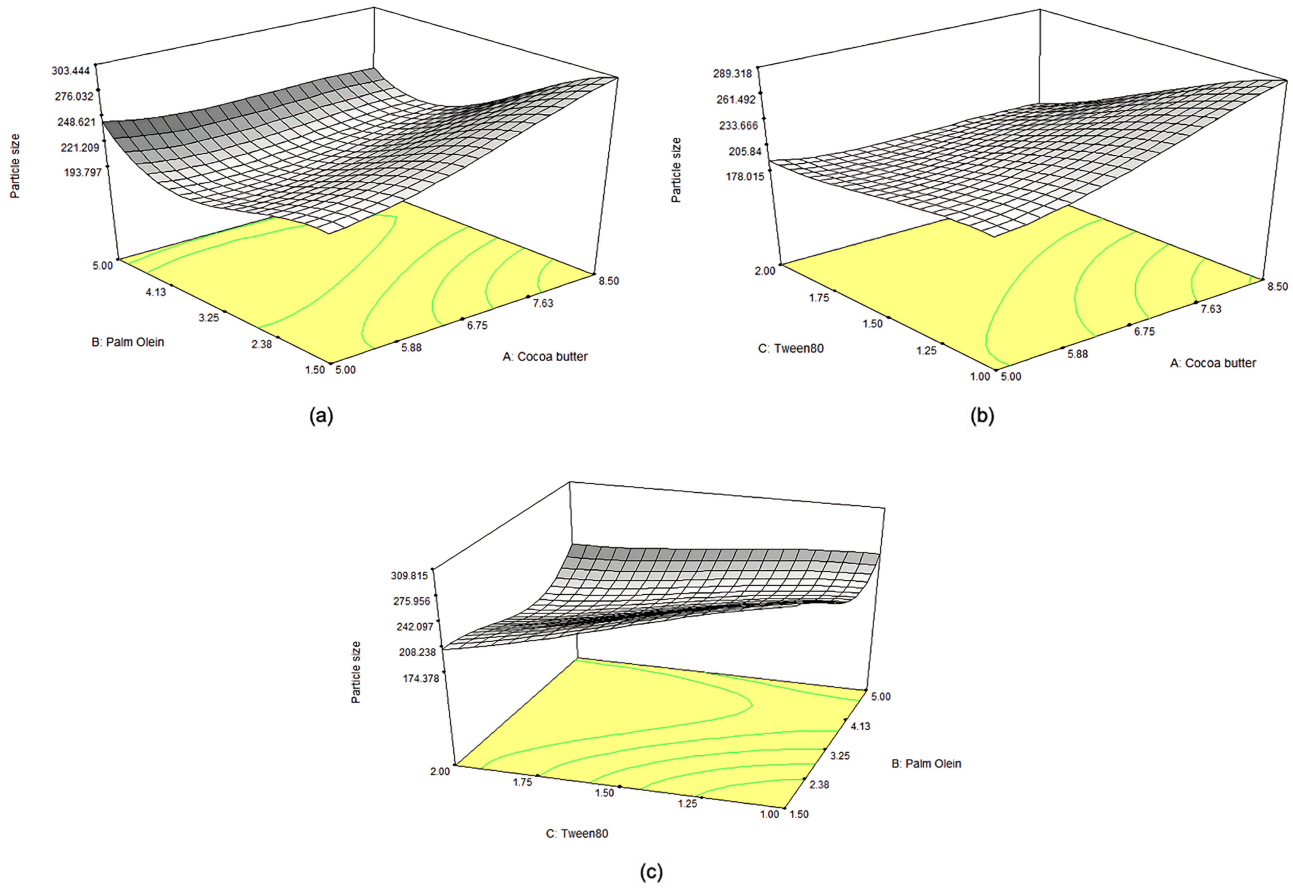

Figure 2 Response surface plots of the interaction on the particle size (nm) between **(a)** the mass of cocoa butter and palm oil with constant mass of 1.5g of Tween 80, **(b)** the mass of cocoa butter and tween 80 with a fixed amount of 3.25g palm oil, **(c)** the mass of palm oil and tween 80 with a fixed amount of 6.75g of cocoa butter.

surface tension of the lipid phase, leading to the formation of smaller-sized particles.[36] Moreover, the surfactant reduced the dispersion viscosity. This was observed in Figure 3c, when the mass of both palm oil and Tween 80 increased, and the interactions between the molecules became more favorable, resulting in a narrow particle size distribution. Tween 80 in this formulation also acted as a stabilizer that helped decrease the variability of the particle sizes and shapes; hence, exhibited a low polydispersity index.[30]

Influence of the Independent Variables on the Zeta Potential

Figure 4 shows the 3D response plots for the interaction between the independent variables and zeta potential. A zeta potential value of more than ±30 mV suggests good dispersion in the nanoformulation systems.[25] Based on the plot (Figure 4a), a more negative zeta potential value was obtained as the mass of liquid lipid increased. The palm oil in the formulation provided a more disoriented environment, which enhanced the mobility of the particles in the dispersion, thus providing more negative zeta potential values. In contrast, shown in Figure 4b, a higher amount of cocoa butter contributed to a more rigid lipid matrix, affecting the interactions of the particles in the dispersion and resulting in variations in the zeta potential values.[34] Moreover, the reduced zeta potential values were due to the presence of Tween 80 as a stabilizer in the NLC system. Although this surfactant is a non-ionic molecule, higher amounts of Tween 80 have been shown to produce a more negative zeta potential, potentially increasing the stability of the dispersion.[34]

Verification of the Final Reduced Model

Based on the final CCD results, the optimum masses of cocoa butter, palm oil, and Tween 80 were calculated automatically using the derived polynomial equations, as shown in Table 3. Five solutions were suggested, and the first solution was selected for validation because it had the highest desirability value of 1.000, as listed in Table 4.

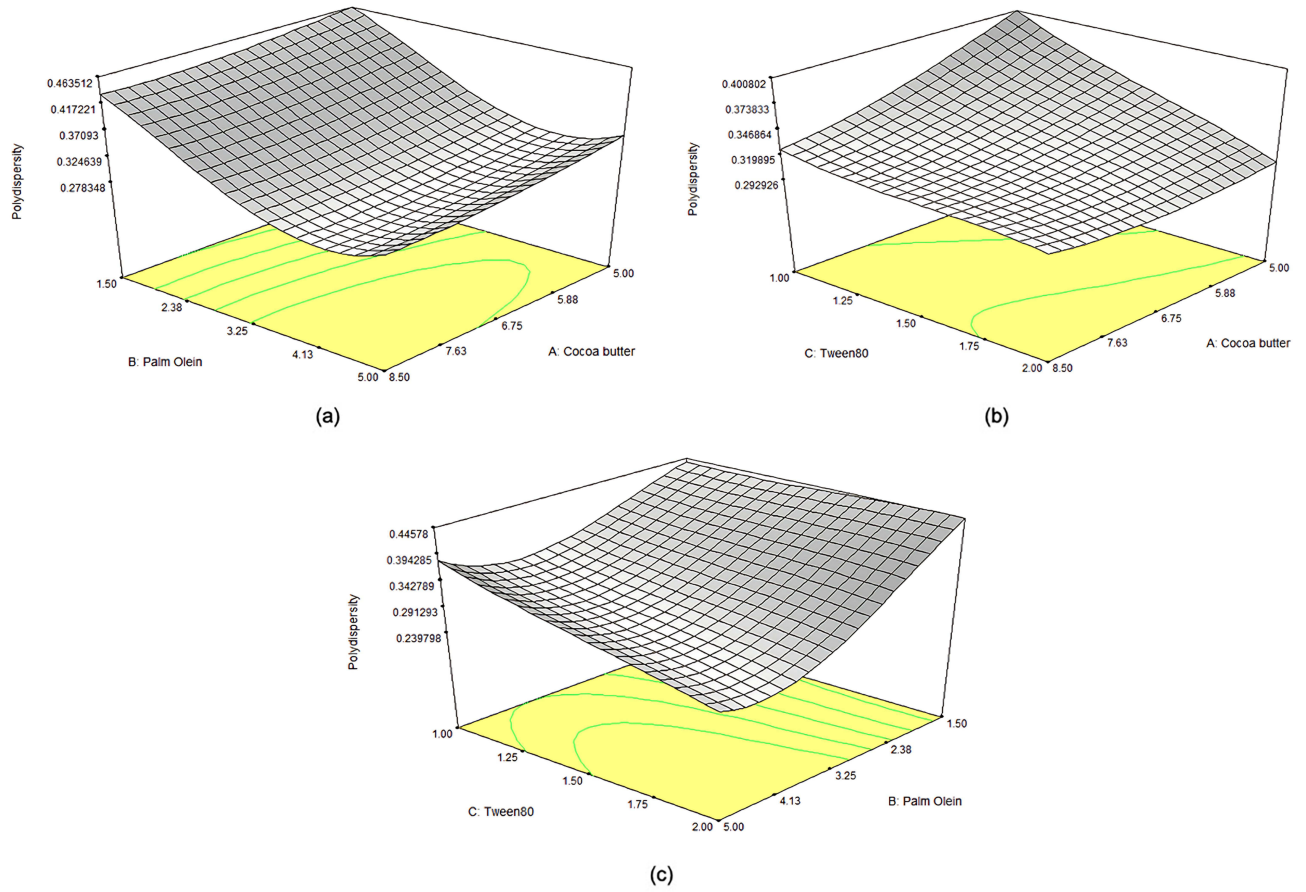

Figure 3 Response surface plots of the interaction on the polydispersity index between **(a)** mass of cocoa butter and palm oil with a fixed amount of 1.5g of Tween 80, **(b)** mass of cocoa butter and Tween 80 with a constant amount of 3.25g of palm oil, and **(c)** mass of palm oil and Tween 80 with a constant amount of 6.75g of cocoa butter.

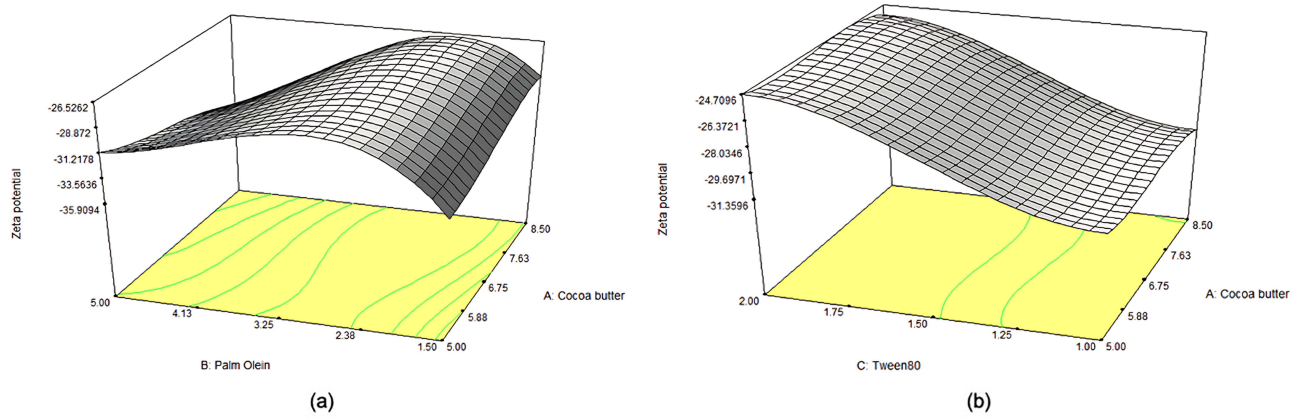

Figure 4 Response surface plots for the effect of interaction on zeta potential between **(a)** mass of cocoa butter and palm oil with fixed 1.5g of Tween 80, and **(b)** mass of cocoa butter and Tween 80 with 3.25g of palm oil.

The experimental values obtained for all responses were close to the predicted values, exhibiting minimal relative error percentages, thereby confirming the validity of the model as shown in Table 5. No significant differences were observed between the predicted values generated by the software based on CCD and experimental values for particle size, polydispersity, and zeta potential, suggesting that the data were in good agreement with the predicted values.

Table 4 Solutions Generated by CCD Following the Final Reduced Model

Solution	Cocoa Butter (g)	Palm Oil (g)	Tween 80 (g)	Desirability
1	6.90	3.00	1.15	**1.000**
2	5.00	5.00	1.46	0.941
3	5.01	5.00	1.46	0.939
4	7.62	4.96	1.08	0.881
5	7.58	4.97	1.09	0.881

Notes: Solution 1 was selected for validation due to its highest desirability value presented in the bold font.

Table 5 The Predicted and Experimental Values for the Optimized NLC

Dependent Variables	Predicted Values	Experimental Values
Particle size (nm)	250	254.42 ± 3.91
Polydispersity index	0.35	0.38 ± 0.01
Zeta potential (mV)	−30	−30.54 ± 0.85

Notes: Data for experimental values were expressed as mean ± SEM.

For astaxanthin-loaded NLC, the mean particle size, polydispersity index and zeta potential were 246.50 ± 3.22 nm, 0.38 ± 0.01 and −30.30 ± 0.52 mV, respectively. The mean particle size of the astaxanthin-loaded NLC was slightly larger than that of the blank NLC, indicating that astaxanthin was successfully incorporated into NLC.[37] The successful incorporation of astaxanthin into NLC was further confirmed by transmission electron microscopy (TEM) and entrapment efficiency analysis.

Transmission Electron Microscopy

TEM images of the astaxanthin-loaded NLC and blank NLC are shown in Figure 5. Blank NLC (Figure 5a) showed a spherical structure with a size of 183.48 nm, which is within the range reported by DLS. The size of astaxanthin-loaded NLC in Figure 5b was 317.92 nm, which was larger than that of the blank NLC, indicating that astaxanthin was successfully loaded into the NLC, consistent with previous study by Hu. F et al (2019), which also reported that astaxanthin-loaded poly(lactic-co-glycolic acid) (PLGA) nanoparticles (NP) had a larger particle size observed under TEM compared to the blank PLGA NP.[29] The observed discrepancy in the particle size measured using TEM and DLS

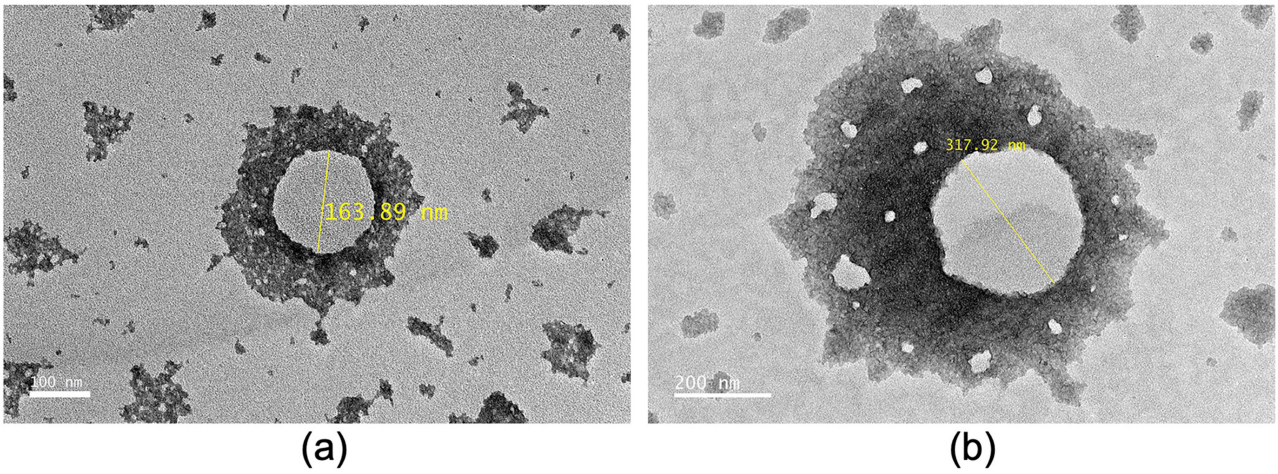

Figure 5 Transmission electron microscopy images of **(a)** blank NLC, and **(b)** astaxanthin-loaded NLC.

https://doi.org/10.2147/IJN.S544064

methods may be due to the operational principles of both techniques.[18] DLS measures the hydrodynamic diameter, which is the size of a particle, including its dissolved solution and potential aggregation, whereas TEM measures the physical size of an individual particle.[38] Thus, TEM provided a more accurate representation of the nanoparticle size, whereas the nanoparticle size reported by DLS was larger owing to the influence of the surrounding medium and particle interactions.

Entrapment Efficiency

The entrapment efficiency of astaxanthin-loaded NLC was 99.69 ± 0.0003% (n=3). This result demonstrated a remarkably high entrapment efficiency, indicating that astaxanthin was effectively encapsulated in the NLC. This can be attributed to the lipid matrix of the NLC, which allows favorable interactions with the hydrophobic nature of astaxanthin, warranting the compound to remain within the NLC system.[39] Additionally, the presence of solid and liquid lipid mixtures in the NLC formulation contributes to an imperfect lattice arrangement that can incorporate a higher amount of astaxanthin and minimize leakage, in addition to enhancing the overall stability of the encapsulated astaxanthin.[20,40]

Storage Stability Determination

The particle size, polydispersity index and zeta potential of the blank NLC and astaxanthin-loaded NLC dispersions stored at refrigerated, room and accelerated temperatures were presented in Figure 6. The particle size of dispersions of blank NLC and astaxanthin-loaded NLC showed stability and expressed minimal changes except for blank NLC in the

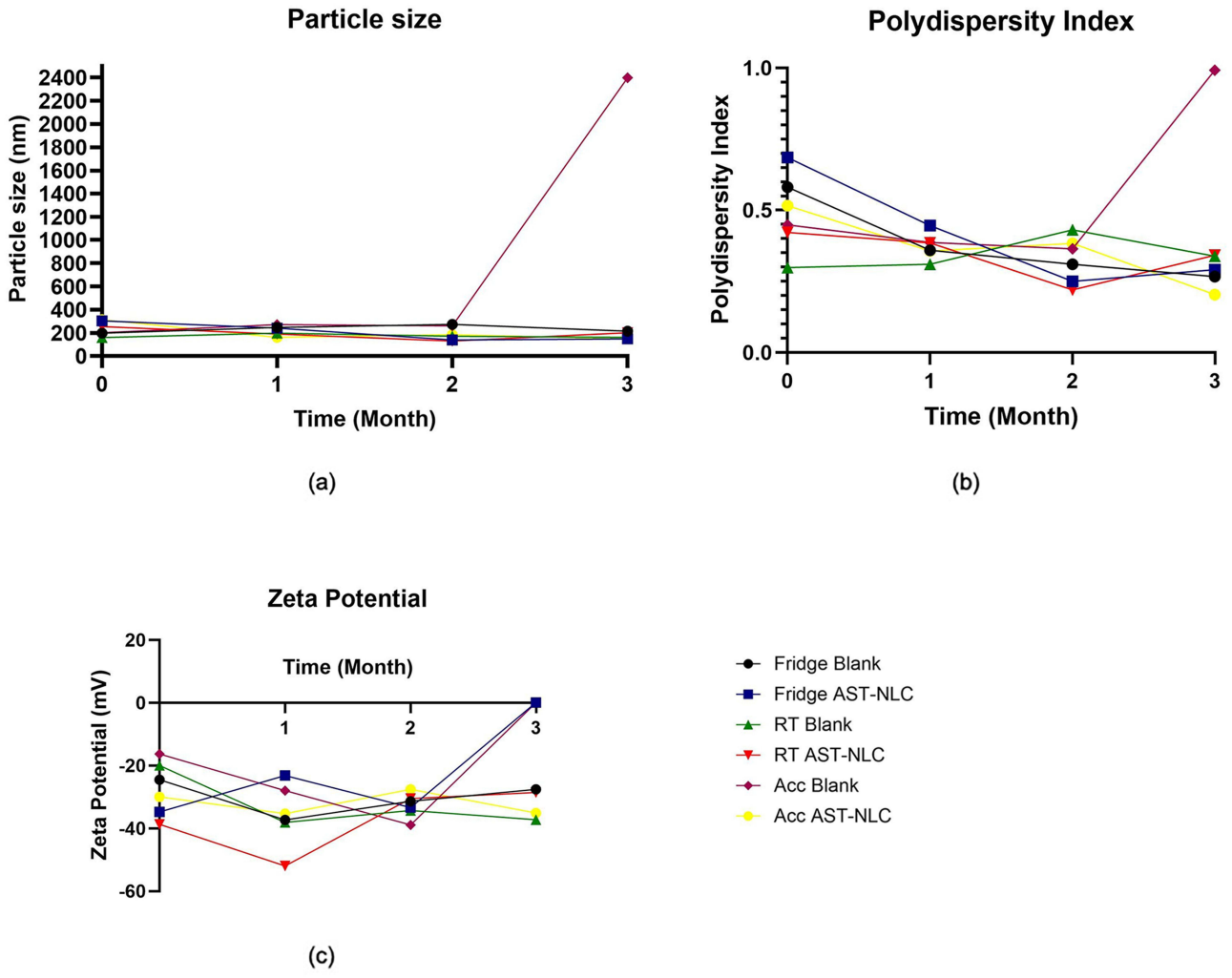

Figure 6 The changes in particle size **(a)**, polydispersity index **(b)** and zeta potential **(c)** of the formulation in 3 months storage.

accelerated condition where the size increased dramatically in the third month (Figure 6a). As suspected, the polydispersity index of blank NLC in the extreme temperature would also follow the trend, with a spike in the polydispersity index as seen in Figure 6b. Similarly, Hassan et al (2021) also reported that the particle size and polydispersity index of their formulation increased dramatically at 3 months storage under an extreme condition (40 ± 2 °C).[21] This shows that accelerated condition is not suitable for the storage of lipid based nanoparticles. The surface charge of blank NLC in accelerated condition and refrigerated astaxanthin-loaded NLC showed positive values (+0.01 and +0.07 mV) in Figure 6c. Higher temperature in an accelerated condition tends to increase the kinetic energy of the particles, thus, reducing the stability of the sample.[41,42] For astaxanthin-loaded NLC in 4°C, the positive zeta potential value may be due to interaction of astaxanthin with the lipid matrix over time, reducing the surface charge.[19,20]

Conclusion

The optimum composition of cocoa butter, palm oil, and Tween 80 for the formulation was obtained from CCD in RSM, and the formulation showed no significant difference between the expected and experimental values. Astaxanthin-loaded NLC showed high entrapment efficiency, suggesting that NLC could be potential carriers for enhancing the bioavailability of astaxanthin. Future research will be focusing on demonstrating the functional advancements by characterizing the optimized astaxanthin-loaded NLC based on thermal, molecular, crystalline analyses as well as in vitro drug release and in vivo pharmacokinetics profile study. Obtaining insights into these properties can also help in designing an improved formulation to enhance the oral bioavailability of astaxanthin.

Abbreviations

NLC, nanostructured lipid carriers; RSM, Response Surface Methodology; CCD, Central Composite design; COX-2, cyclooxygenase 2; C_{max}, maximum plasma concentration; GRAS, Generally Recognized as Safe; SLN, solid lipid nanoparticles; TRF, tocotrienol-rich fraction; OFAT, One Factor At a Time; PdI, polydispersity index; DLS, dynamic light scattering; TEM, transmission electron microscopy; EE, entrapment efficiency; SEM, standard error of mean; ANOVA, Analysis of Variance; 3D, three-dimensional; PLGA, poly(lactic-co-glycolic acid); NP, nanoparticles.

Acknowledgments

The authors acknowledge Fuji Chemicals Industry Co., Ltd. (Japan) for their thoughtful gift the AstaReal® L10 samples used in this study, distributed by Elite Organic Sdn Bhd (Kuala Lumpur, Malaysia). The authors are also grateful for the sponsorship of the cocoa butter by the Guan Chong Cocoa Manufacturing Sdn Bhd (Johor, Malaysia). The authors would also like to express their acknowledgement to the Institute Bioscience, Universiti Putra Malaysia, for the TEM analysis.

Funding

This work was supported by the Fundamental Research Grant Scheme (FRGS), grant number FRGS/1/2021/STG01/UPM/02/14, from the Ministry of Higher Education Malaysia. The sponsor had no such involvement in this study.

Disclosure

Ms Nur Rafiqah Abdol Wahab reports grants from Ministry of Higher Education of Malaysia (Fundamental Research Grant Scheme), during the conduct of the study. Dr Haniza Hassan reports grants from Ministry of Higher Education Malaysia (Fundamental Research Grant Scheme), during the conduct of the study. The author(s) report no conflicts of interest in this work.

References

1. Fan KW, Chen F. Production of high-value products by marine microalgae thraustochytrids. In: *Bioprocessing for Value-Added Products From Renewable Resources*. Elsevier: 2007:293–323. doi:10.1016/B978-044452114-9/50012-8
2. Abdol Wahab NR, Meor Mohd Affandi MMR, Fakurazi S, Alias E, Hassan H. Nanocarrier system: state-of-the-art in oral delivery of astaxanthin. *Antioxidants*. 2022;11(9):1676. doi:10.3390/antiox11091676
3. Davan I, Fakurazi S, Alias E, Ibrahim N, Izzah Hwei NM, Hassan H. Astaxanthin as a potent antioxidant for promoting bone health: an up-to-date review. *Antioxidants*. 2023;12(7):1–26. doi:10.3390/antiox12071480

4. Sekikawa T, Kizawa Y, Li Y, Takara T. Cognitive function improvement with astaxanthin and tocotrienol intake: a randomized, double-blind, placebo-controlled study. *J Clin Biochem Nutr*. 2020;67(3):307–316. doi:10.3164/jcbn.19-116
5. Zhuge F, Ni Y, Wan C, Liu F, Fu Z. Anti-diabetic effects of astaxanthin on an stz-induced diabetic model in rats. *Endocr J*. 2021;68(4):451–459. doi:10.1507/endocrj.EJ20-0699
6. Chang HI, Shao CW, Huang E, Huang KY. Development of astaxanthin-loaded nanosized liposomal formulation to improve bone health. *Pharmaceuticals*. 2022;15(4). doi:10.3390/ph15040490
7. Odeberg JM, Lignell Å, Pettersson A, Höglund P. Oral bioavailability of the antioxidant astaxanthin in humans is enhanced by incorporation of lipid based formulations. *Eur J Pharm Sci*. 2003;19(4):299–304. doi:10.1016/S0928-0987(03)00135-0
8. Osterlie MBB, Østerlie M, Bjerkeng B. Plasma appearance and distribution of astaxanthin E/Z and R/S isomers in plasma lipoproteins of men after single dose administration of astaxanthin. *J Nutr Biochem*. 2000;2863(00):482–490. doi:10.1016/s0955-2863(00)00104-2
9. Okada Y, Ishikura M, Maoka T. Bioavailability of astaxanthin in haematococcus algal extract: the effects of timing of diet and smoking habits. *Biosci Biotechnol Biochem*. 2009;73(9):1928–1932. doi:10.1271/bbb.90078
10. Date AA, Hanes J, Ensign LM. Nanoparticles for oral delivery: design, evaluation and state-of-the-art. *J Control Release*. 2016;240(12):504–526. doi:10.1016/j.jconrel.2016.06.016
11. Jeevanandam J, Chan YS, Danquah MK. Nano-formulations of drugs: recent developments, impact and challenges. *Biochimie*. 2016;128-129:99–112. doi:10.1016/j.biochi.2016.07.008
12. Khan S, Baboota S, Ali J, Khan S, Narang RS, Narang JK. Nanostructured lipid carriers: an emerging platform for improving oral bioavailability of lipophilic drugs. *Int J Pharm Investig*. 2015;5(4):182–191. doi:10.4103/2230-973X.167661
13. Elmowafy M, Ibrahim HM, Ahmed MA, Shalaby K, Salama A, Hefesha H. Atorvastatin-loaded nanostructured lipid carriers (Nlcs): strategy to overcome oral delivery drawbacks. *Drug Deliv*. 2017;24(1):932–941. doi:10.1080/10717544.2017.1337823
14. Naseri N, Valizadeh H, Zakeri-Milani P. Solid lipid nanoparticles and nanostructured lipid carriers: structure, preparation and application. *Adv Pharm Bull*. 2015;5(3):305–313. doi:10.15171/apb.2015.043
15. Talegaonkar S, Bhattacharyya A. Potential of lipid nanoparticles (SLNs and NLCs) in enhancing oral bioavailability of drugs with poor intestinal permeability. *AAPS Pharm Sci Tech*. 2019;20(3). doi:10.1208/s12249-019-1337-8
16. Efendy Goon D, Sheikh Abdul Kadir SH, Latip NA, Rahim S, Mazlan M. Palm oil in lipid-based formulations and drug delivery systems. *Biomolecules*. 2019;9(2):64. doi:10.3390/biom9020064
17. Bratu A, Ott C, Balanuca B, Badea N, Lacatusu I. The association effect of cocoa butter with vegetable oils on the obtaining of lipid nanocarriers loaded with antidepressant and antipsychotic drugs. *Rev Roum Chim*. 2020;65(1):57–67. doi:10.33224/rrch.2020.65.1.06
18. Tamjidi F, Shahedi M, Varshosaz J, Nasirpour A. Design and characterization of astaxanthin-loaded nanostructured lipid carriers. *Innov Food Sci Emerg Technol*. 2014;26:366–374. doi:10.1016/j.ifset.2014.06.012
19. Radić K, Barbosa AI, Reis S, Marijan M, Costa Lima SA, Čepo DV. Preparation of astaxanthin/zeaxanthin-loaded nanostructured lipid carriers for enhanced bioavailability: characterization-, stability- and permeability study. *Acta Pharm*. 2023;73(4):581–599. doi:10.2478/acph-2023-0038
20. Hassan H, Adam SK, Alias E, Affandi MMRMM, Shamsuddin AF, Basir R. Central composite design for formulation and optimization of solid lipid nanoparticles to enhance oral bioavailability of Acyclovir. *Molecules*. 2021;26(18). doi:10.3390/molecules26185432
21. Mohd Zaffarin AS, Ng SF, Ng MH, Hassan H, Alias E. Development and optimization of nano-hydroxyapatite encapsulating tocotrienol-rich fraction formulation using response surface methodology. *Pharmaceutics*. 2025;17(1). doi:10.3390/pharmaceutics17010010
22. Bhattacharya S. Central composite design for response surface methodology and its application in pharmacy. In: *Response Surface Methodology in Engineering Science*. IntechOpen; 2021. doi:10.5772/intechopen.95835
23. Alam T. Quality by design based development of nanostructured lipid carrier: a risk based approach. *Explor Med*. 2022;3(6):617–638. doi:10.37349/emed.2022.00118
24. Mall J, Naseem N, Haider MF, Rahman MA, Khan S, Siddiqui SN. Nanostructured lipid carriers as a drug delivery system: a comprehensive review with therapeutic applications. *Intell Pharm*. 2025;3(4):243–255. doi:10.1016/j.ipha.2024.09.005
25. Rohmah M, Raharjo S, Hidayat C, Martien R. Application of response surface methodology for the optimization of β-Carotene-loaded nanostructured lipid carrier from mixtures of palm stearin and palm olein. *J Am Oil Chem Soc*. 2020;97(2):213–223. doi:10.1002/aocs.12310
26. Choi HD, Kang HE, Yang SH, Lee MG, Shin WG. Pharmacokinetics and first-pass metabolism of astaxanthin in rats. *Br J Nutr*. 2011;105(2):220–227. doi:10.1017/S0007114510003454
27. Chik MW, Affandi MMRMM, Chellammal HSJ, Hazalin NAMN, Singh GKS. Astaxanthin nanoemulsion and nanoparticle formulations and their therapeutic potential: a review. *Adv Pharmacol Pharm*. 2025;13(3):342–354. doi:10.13189/app.2025.130306
28. Santonocito D, Raciti G, Campisi A, et al. Astaxanthin-loaded stealth lipid nanoparticles (AST-SSLN) as potential carriers for the treatment of alzheimer's disease: formulation development and optimization. *Nanomaterials*. 2021;11(2):1–17. doi:10.3390/nano11020391
29. Hu F, Liu W, Yan L, Kong F, Wei K. Optimization and characterization of poly(lactic-co-glycolic acid) nanoparticles loaded with astaxanthin and evaluation of anti-photodamage effect in vitro. *R Soc Open Sci*. 2019;6(10). doi:10.1098/rsos.191184
30. Hu Q, Hu S, Fleming E, Lee JY, Luo Y. Chitosan-caseinate-dextran ternary complex nanoparticles for potential oral delivery of astaxanthin with significantly improved bioactivity. *Int J Biol Macromol*. 2020;151:747–756. doi:10.1016/j.ijbiomac.2020.02.170
31. Akhoond Zardini A, Mohebbi M, Farhoosh R, Bolurian S. Production and characterization of nanostructured lipid carriers and solid lipid nanoparticles containing lycopene for food fortification. *J Food Sci Technol*. 2018;55(1):287–298. doi:10.1007/s13197-017-2937-5
32. Hassan H, Bello RO, Adam SK, et al. Acyclovir-loaded solid lipid nanoparticles: optimization, characterization and evaluation of its pharmacokinetic profile. *Nanomaterials*. 2020;10(9):1–17. doi:10.3390/nano10091785
33. Shah R, Eldridge D, Palombo E, Harding I. Optimisation and stability assessment of solid lipid nanoparticles using particle size and zeta potential. *J Phys Sci*. 2014;25(1):59–75.
34. Shtay R, Tan CP, Schwarz K. Development and characterization of solid lipid nanoparticles (SLNs) made of cocoa butter: a factorial design study. *J Food Eng*. 2018;231:30–41. doi:10.1016/j.jfoodeng.2018.03.006
35. Anarjan N, Nehdi IA, Tan CP. Influence of astaxanthin, emulsifier and organic phase concentration on physicochemical properties of astaxanthin nanodispersions. *Chem Cent J*. 2013;7(1). doi:10.1186/1752-153X-7-127
36. Hu FQ, Jiang SP, Du YZ, Yuan H, Ye YQ, Zeng S. Preparation and characterization of stearic acid nanostructured lipid carriers by solvent diffusion method in an aqueous system. *Colloids Surf B Biointerfaces*. 2005;45(3–4):167–173. doi:10.1016/j.colsurfb.2005.08.005

37. Anwar W, Dawaba H, Afouna M, Samy A, Rashed M, Abdelaziz A. Enhancing the oral bioavailability of candesartan cilexetil loaded nanostructured lipid carriers: in vitro characterization and absorption in rats after oral administration. *Pharmaceutics*. 2020;12(11):1047. doi:10.3390/pharmaceutics12111047
38. Filippov SK, Khusnutdinov R, Murmiliuk A, et al. Dynamic light scattering and transmission electron microscopy in drug delivery: a roadmap for correct characterization of nanoparticles and interpretation of results. *Mater Horizons*. 2023;10(12):5354–5370. doi:10.1039/d3mh00717k
39. Zhihrotulwida D, Rosita N, Soeratri W. Development of astaxanthin-loaded nanostructured lipid carriers using a combination of cetyl palmitate and soybean oil. *J Res Pharm*. 2024;28(6):2038–2045. doi:10.29228/jrp.878
40. Nguyen VH, Thuy VN, Van TV, Dao AH, Lee BJ. Nanostructured lipid carriers and their potential applications for versatile drug delivery via oral administration. *OpenNano*. 2022;8(August):100064. doi:10.1016/j.onano.2022.100064
41. Feng S, Tian Y, Sheng J, et al. Enhancing high-temperature stability of limonene-loaded nanostructured lipid carriers with various solid lipids. *Food Bioeng*. 2024;3(3):323–336. doi:10.1002/fbe2.12101
42. Shamsuddin NAM, Azmi F, Husain K, Mun LL, Zulfakar MH. Design and characterisation of curcumin-loaded nanostructured lipid carriers for safe and efficient topical drug delivery in the treatment of pressure ulcer. *Sains Malays*. 2024;53(6):1343–1362. doi:10.17576/jsm-2024-5306-10